

LOW-MAGNITUDE SEISMICITY OF THE CONTINENT-OCEAN TRANSITION ZONE IN THE EURASIAN ARCTIC

A. N. Morozov^{1,2,3} , N. V. Vaganova² , Ya. V. Konechnaya^{2,4} , Ya. A. Mikhailova² , and N. V. Petrova⁴ 

¹Schmidt Institute of Physics of the Earth of the Russian Academy of Sciences, Moscow, Russia

²N. Laverov Federal Center for Integrated Arctic Research of the Ural Branch of the Russian Academy of Sciences, Arkhangelsk, Russia

³Geophysical Center of the Russian Academy of Sciences, Moscow, Russia

⁴Geophysical Survey of the Russian Academy of Sciences; Obninsk, Russia

* **Correspondence to:** Alexey Morozov, morozovalexey@yandex.ru

Abstract: A significant increase in the number of seismic stations occurred in the Eurasian Arctic during the late 20th to early 21st century, which led to a decrease in the minimum magnitude of earthquake registration for some Arctic regions. One of the areas that have been until recently poorly studied in terms of low-magnitude seismicity includes the continent-ocean transition zone in the northern Eurasian shelf. An analysis of the monitoring performed using the seismic stations in operation in the Franz Josef Land and Severnaya Zemlya archipelagos complemented with data from the seismic stations on the Svalbard archipelago for the period from December 2011 to November 2020 made it possible to study the space-time patterns in the low magnitude seismicity at the continent-ocean transition zone. The most active features are the Franz Victoria and St. Anna grabens, and the Bely and Victoria High.

Keywords: continent-ocean transition zone, continental slope, Eurasian Arctic, seismicity.

Citation: Morozov, A. N., N. V. Vaganova, Ya. V. Konechnaya, Ya. A. Mikhailova, and N. V. Petrova (2024), Low-Magnitude Seismicity of the Continent-Ocean Transition Zone in the Eurasian Arctic, *Russian Journal of Earth Sciences*, 24, ES4011, EDN: PRLQWW, <https://doi.org/10.2205/2024es000927>

Introduction

The start of seismological observations in the Arctic dates back to 1906 when seismological observations began in Vassijaure, northern Sweden. The Vassijaure seismic station was the first to be operated north of the Arctic Circle. The station was equipped with a horizontal Wiechert instrument which was subsequently, in 1915, transferred to the Abisko Research Station [Avetisov, 1996; Kulhánek, 1988]. However, the first important data on the seismicity of the Arctic territories in the early twentieth century was given by the Disko (Godhavn) seismic station, which operated from October 1907 to 1912 on Disko Island off the west coast of Greenland [Harboe, 1911], as well as studies of regional seismicity in the area of the Svalbard archipelago, which were carried out under the direction of G. Rempp from November 1911 to 1912 [Rempp, 1914].

The total number of seismic stations north of the Arctic Circle has been gradually, and at variable rates, increasing. However, until the beginning of the 21st century, the extensive Arctic territory was extremely unevenly covered by stations because of a severe climate and unfavorable geographic conditions (Figure 1a). As a result, the minimum magnitude of completeness varied widely over the Arctic region, from 2.0–2.5 for northern Scandinavia to as high as 4.0 in some areas, such as eastern part of the mid-oceanic Gakkel Ridge [Avetisov, 1996; Engen et al., 2003].

However, this was sufficient to get a good general notion of the seismicity in the main seismic zones of the Arctic, viz., the spreading boundary between the North American and Eurasian plates. The boundary runs from Iceland through the Eurasian Basin, and the Laptev Sea shelf as far as Northeast Eurasia. However, the total number of stations and

RESEARCH ARTICLE

Received: 5 March 2024

Accepted: 30 July 2024

Published: 10 December 2024



Copyright: © 2024. The Authors. This article is an open access article distributed under the terms and conditions of the Creative Commons Attribution (CC BY) license (<https://creativecommons.org/licenses/by/4.0/>).

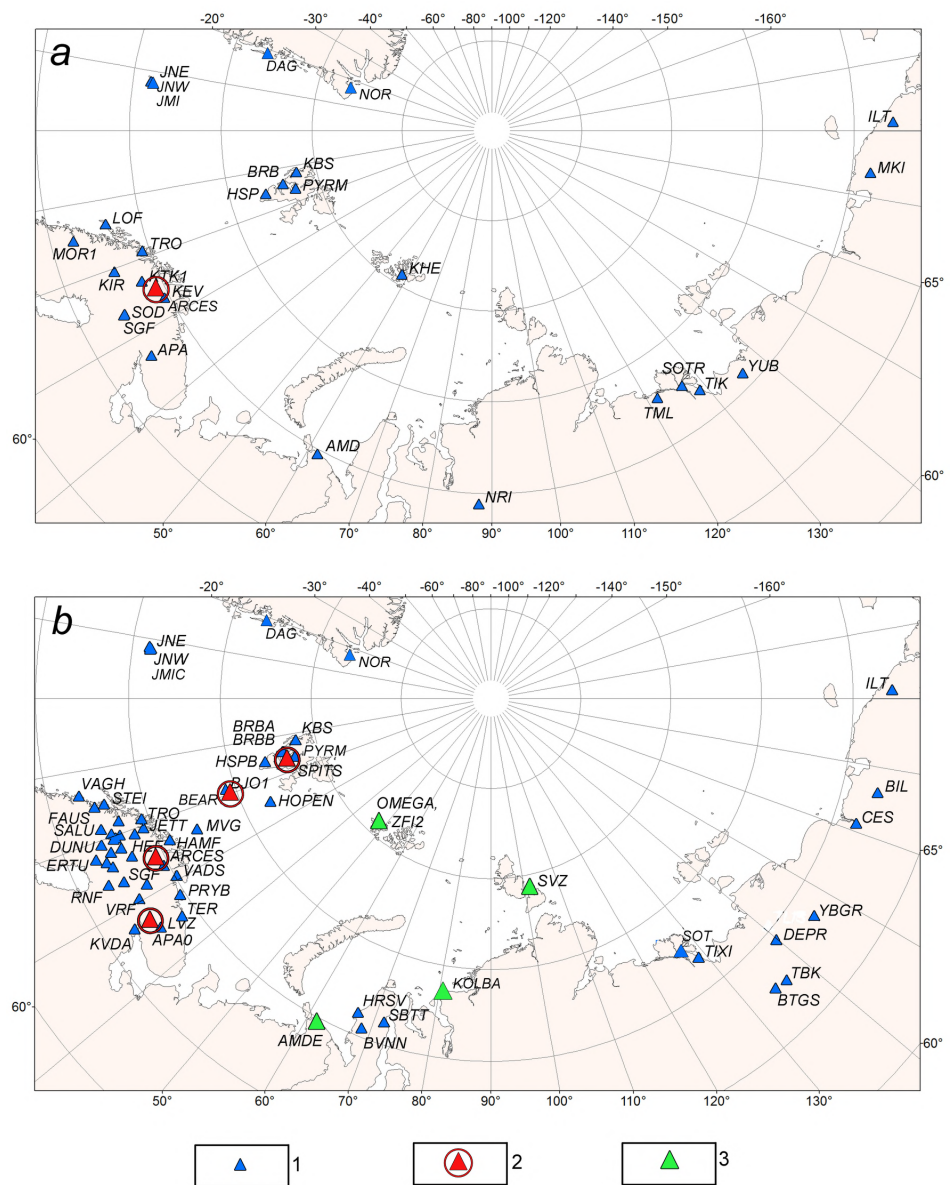


Figure 1. Map of seismic stations in the Eurasian Arctic, operating in the 80s of the XX century (a) and at the time of 2019 (b): 1 – seismic stations of the GE network (GEOFON Global Seismic Network), NO network (NORSAR Station Network), NS network (University of Bergen Seismic Network), and PL network (Polish Seismic Network) by [FDSN, 2024]; 2 – seismic arrays of the NO network; 3 – seismic stations of the AH network (Arkhangelsk Seismic Network) by [FDSN, 2024].

their density was quite insufficient for detailed studies of seismicity in some Arctic areas [Avetisov, 1996]. As a result, it was not possible to register low-magnitude earthquakes for some areas of the Arctic. The study of low-magnitude earthquakes provides much evidence from which to infer space-time variations of seismicity and to the geodynamic processes in that area [Panasenko, 1986].

The number of seismic stations in the Eurasian Arctic considerably increased in the late 20th to early 21st century. The stations were equipped with advanced sensitive instruments, reducing the lower magnitude of complete reporting for some Arctic areas (Figure 1b). The use of new seismic stations and improved algorithms for seismic signal processing and earthquake location gave more knowledge of seismicity both for the Arctic as a whole and for individual areas [Antonovskaya et al., 2020; Gibbons et al., 2017; Morozov et al., 2016; Rogozhin et al., 2016; Schweitzer et al., 2021].

The areas that until recently were poorly studied in terms of low-magnitude seismicity include the continent-ocean transition zone in the northern Eurasian shelf. The research of the spatial distribution of seismicity in this area is important and topical. In the first place, in virtue of its geographic and climate conditions, the region remains poorly studied so far. Secondly, the incoming seismic data in combination with available geophysical information shed new light on the geodynamics of the region.

Previously [Morozov *et al.*, 2014] we did a preliminary analysis of seismicity occurring in the continent-ocean transition zone of the Barents-Kara region in the Arctic. However, that analysis was based on the data of a single station ZFI2 (AH network by [FDSN, 2024]) with additional data from stations in the Svalbard archipelago. The study covers period from December 2011 to January 2014. Subsequently, new seismic stations were installed on Franz Josef Land and in Severnaya Zemlya (AH network by [FDSN, 2024]) (Figure 1b), considerably expanding the area of study and providing seismic data for the period from December 2011 to November 2020 (Figure 2). This article presents the results of registration, location and analysis of the spatial-temporal distribution of low-magnitude earthquakes within the continent-ocean transition zone in the Eurasian Arctic.

Description of Data Set and Methods

The area of study is the northern part of the Arctic Eurasian shelf (Figure 2). The seismic monitoring of the study area was based on data coming from the AH network [FDSN, 2024] stations operated on Franz Josef Land (ZFI and OMEGA) and Severnaya Zemlya (SVZ) for the period from October 2011 to November 2020. Their frequency characteristics are shown in Figure 3. Seismic stations are located on Arctic islands, so their frequency characteristics can vary greatly depending on the season. For example, in the winter months, the sea area is under ice cover and economic activity on the islands sharply decreases, which is reflected in the frequency characteristics of seismic stations.

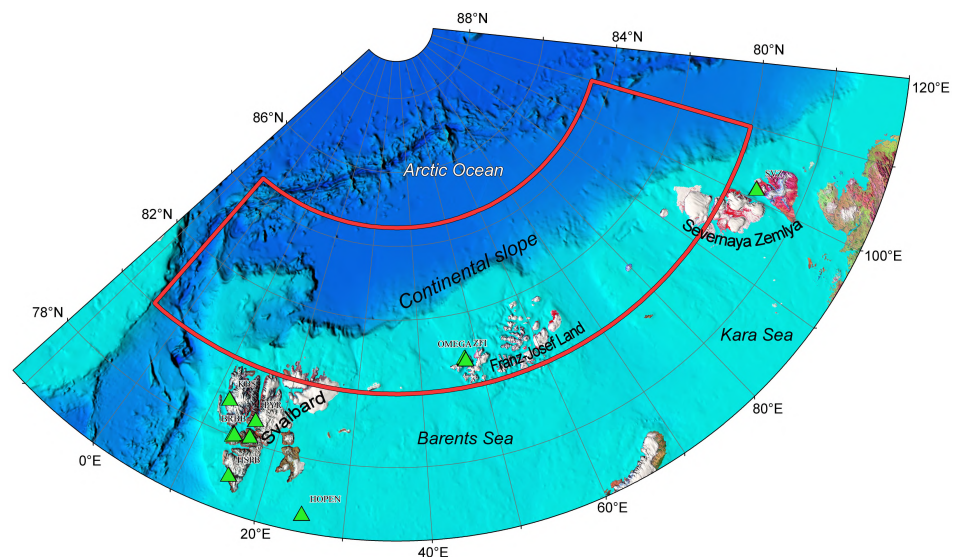


Figure 2. Map showing the boundaries of the area of study (red line) and location of seismic stations (green triangles).

We minimized the epicenter location uncertainty by also using waveform data recorded by the stations operated on Svalbard and in northern Scandinavia. These are KBS of the GE network (GEOFON, Global Seismic Network), HSPB of the PL network (Polish Seismic Network), HOPEN and BJO1 of the NS network (Norwegian National Seismic Network University of Bergen Norway), as well as the SPA0 stations in the SPITS seismic array (NORSAR Station Network) [FDSN, 2024]. Data access was via the electronic resource GEOFON [GFZ German Research Center for Geosciences, 2021]. If the earthquakes were also

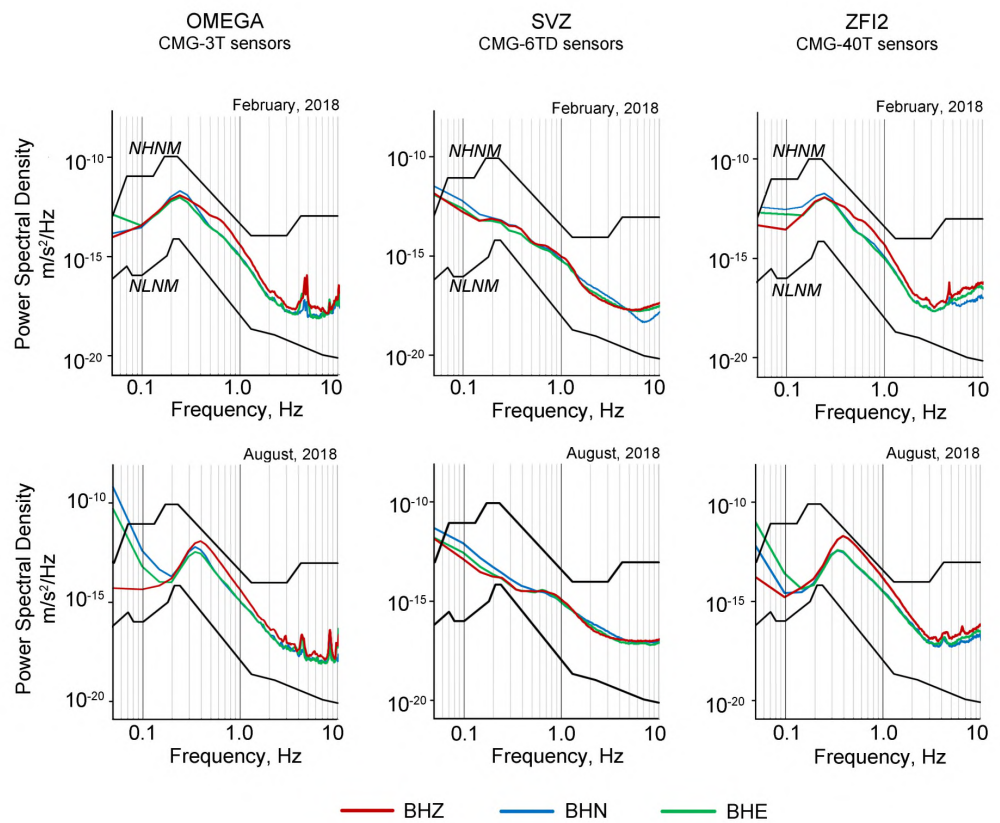


Figure 3. Power spectral density for seismic stations calculated from BHZ, BHN, and BHE components of the seismic stations. The New High and New Low Noise Models (NHNM and NLNM) are marked by black lines [Peterson, 1993].

recorded by remote seismic stations, then we took the arrival times of these stations from the International Seismological Centre [International Seismological Centre, 2024].

As mentioned above, at the present time, the number of permanent seismic stations in the Eurasian Arctic is the greatest for the entire period of instrumental observation. However, the conditions are still unfavorable for reliable epicenter location, especially as concerns low-magnitude earthquakes. The reasons for this are low number of stations, the great interstation distances, and their location in space relative to the epicenter of the arctic earthquakes. For the continental slope between the archipelagos of Svalbard and Franz Josef Land, earthquakes were located under conditions when seismic stations were located to the west and east of the earthquake epicenters (Figure 2, see also Figure 5). On the contrary, within the continental slope between the archipelagos of Franz Josef Land and Severnaya Zemlya until 2016, the location of earthquakes occurred in a narrow azimuthal coverage. After the start of operation of the SVZ seismic station (AH network by [FDSN, 2024] in 2016 it became possible to locate earthquakes according to stations located in the west and east relative to the epicenters.

Earthquakes that occurred in the study area during the period from October 2011 to November 2020 were recorded by a different number of seismic stations. One part of the earthquakes was recorded by three or more stations, and the other part by only two stations. Some earthquakes were recorded by only one single seismic station.

To locate earthquakes that were recorded by three or more stations, we used the algorithm of the NAS program (New Association System) [Asming et al., 2016; Fedorov et al., 2019], which implements the Generalized beamforming method [Kværna and Ringdal, 1996]. The algorithm calculates error ellipses based on the assumption that the velocity model error estimate is $\Delta v = 0.15 \text{ km/s}$, and the seismic phase arrival time measurement

error estimate is $\Delta t = 0.3$ s (level of confidence is 0.95). Because the stations were remote and few, it has not been possible to find the depths of focus, so the calculation was based on a fixed depth of 5 km.

To locate earthquakes that were recorded by only two stations, we used the “circle and chord” method [Havskov et al., 2002] implemented in WSG (Windows Seismic Grafer) program developed by the Geophysical Survey of the Russian Academy of Sciences (GS RAS) [Akimov and Krasilov, 2020]. This method draws circles with the center at the station locations and the radii equal to the epicentral distances calculated from the S - P times. The calculation of epicenter parameters was also based on a fixed depth of 5 km. The WSG program does not implement error ellipse calculation. We estimate a formal location error of at least 30 km for the study area.

For earthquakes that were recorded by only one single seismic station, we used the algorithm of the EL (Event Location) program [Kremenetskaya and Asming, 2002]. To locate a seismic event by a single station EL algorithm uses the distance defined by S - P time difference and the backazimuth computed by P wave polarization. The depth is assumed to be 5 km. To minimize the possible uncertainty in the location of such earthquakes, we analyzed only earthquakes with clear arrivals of P and S , i.e., with a high signal/noise ratio. The EL program does not implement error ellipse calculation. We estimate the formal location error ± 35 km for an epicentral distance of 200 km ($h = 5$ km). This surely is a less reliable location method, but it still provides an idea of the epicenter distribution.

Of course, we get very inaccurate location results based on data from only two or one seismic stations and the methods implemented in the WSG and EL programs. But, they allowed us to get a rough idea of the distribution of the epicenters for low-magnitude earthquakes, which were recorded by only one or two stations. And as will be shown below, this distribution in general terms corresponds to the distribution of epicenters calculated on the basis of data from three or more seismic stations.

The earthquake coordinates and origin times were calculated using the NOES velocity model [Morozov and Vaganova, 2017]. The model is based on the crustal velocity structure for the area of the Franz Josef Land Archipelago by receiver functions (Table 1). We calculated the M_L magnitude using the average calibration function for North Eurasia [Gabsatarova, 2006] and implemented in the WSG program [Akimov and Krasilov, 2020].

Table 1. NOES velocity model by [Morozov and Vaganova, 2017]

Depth, km	V_p , km/s	V_s , km/s	Note
0	4.3	2.36	
4	6.1	3.6	
17	6.8	3.94	
30	8.15	4.52	
43	8.25	4.75	
71	8.35	4.81	
> 210	8.37	4.56	from IASP 91

Results

A total of 192 earthquakes have been recorded in the continent-ocean transition zone from October 2011 to November 2020. Only 87 earthquakes were recorded by three or more seismic stations, 36 earthquakes were recorded by two stations. And 69 earthquakes were recorded by only one seismic station.

The M_L magnitudes of the earthquakes vary between 0.7 and 3.9 (Figure 4a). Nearly half of all recorded earthquakes have magnitudes $M_L \leq 2.1$. Those with magnitudes $M_L \geq 3.0$ make up a mere 20% of the total number. It can thus be said that the area of study mostly produces low-magnitude earthquakes.

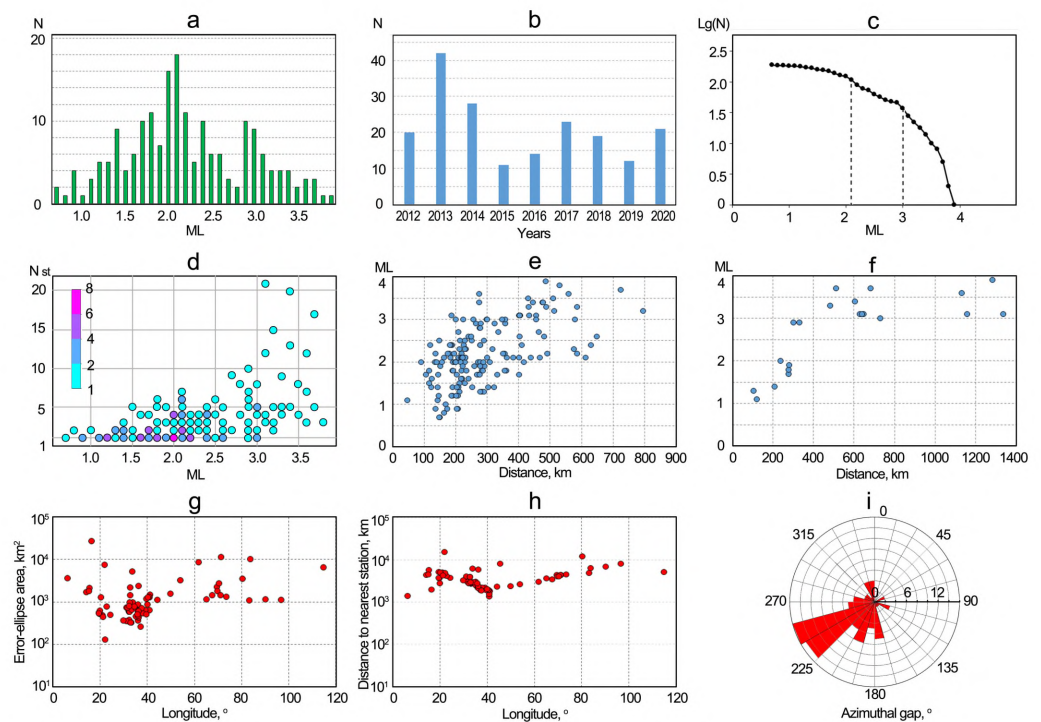


Figure 4. Data analysis of the final catalog of earthquakes: (a) the distribution of the number of recorded earthquakes by their magnitude; (b) the distribution of the number of recorded earthquakes by year; (c) the cumulative frequency-magnitude curve; (d) the number of stations that recorded earthquakes depending on the magnitude (color scale shows the number of earthquakes); (e,f) the distribution of earthquake magnitudes depending on the distance to the seismic station ZFI2 (e) and SVZ (f); (g) the distribution of the area of the earthquake error ellipse depending on latitude; (h) the distribution of distances from earthquake epicenters to the nearest seismic station depending on latitude; (i) the distribution of azimuthal gap values.

However, the functioning of seismic stations on the Franz Josef Land and Severnaya Zemlya archipelagos in different years was affected by technical problems and anthropogenic factors. Technical problems frequently arose at the stations because of extreme conditions in which the instruments were operated. The areas are hardly accessible, so it was impossible to resolve technical problems quickly and take preventive maintenance measures for seismic instrumentation. In addition, increased human activities caused considerable increases in the level of man-induced noise on Alexandra Land (Franz Josef Land archipelago) where seismic instrumentation is installed at the ZFI2 and OMEGA stations (Figure 1b). Therefore, the number of recorded earthquakes and the minimum magnitudes of recorded earthquakes varied greatly depending on the years (Figure 4b). On the diagram of the distribution of the number of recorded earthquakes by their magnitude, we observe several maxima (Figure 4a). In particular, for magnitudes with values of 2.1 and 2.9. For these magnitudes, we also observe inflection points in the cumulative frequency-magnitude curve (Figure 4c).

Figure 4d shows the number of stations that recorded earthquakes depending on the magnitude. Only earthquakes with magnitudes greater than 1.4 could be recorded by three stations. At the same time, some earthquakes with magnitudes up to 3.0 were recorded by only one single station. This is also due to technical problems at the seismic stations closest to such earthquakes.

Figure 4e,f show the distribution of earthquake magnitudes depending on the distance to the seismic station ZFI2 (Figure 4e) and SVZ (Figure 4f). From distances up to 430 km,

the ZFI2 station recorded earthquakes with magnitudes M_L below 2.0, and from distances up to 650 km, earthquakes with magnitudes below 3.0. Within distances up to 340 km, the continental slope falls within the range from 22° E to 70° E. And within distances up to 650 km, practically most of the study area falls in this.

There is not much data for the SVZ seismic station, because the station began to function only in 2016. From distances up to 230 km, the SVZ station recorded earthquakes with magnitudes M_L below 2.0, and from distances up to 330 km, earthquakes with magnitudes below 3.0. Only a small part of the continental slope within our study area falls within these distances. Thus, the capabilities of seismic stations to register low-magnitude earthquakes within the continent-ocean transition zone to the west and east of the Franz Josef Land archipelago were different.

Figure 4g shows the dependence of the area of the error-ellipse on longitude for earthquakes recorded by three or more seismic stations. Overall solution accuracy depends on longitude. The smallest error-ellipses are typical for earthquakes from the region ranging from 20° E to 40° E. This effect is explained by network geometry for this region, reflecting the distance of the located epicenters from the nearest seismic stations (Figure 4h). However, the coverage of the network is unsatisfactory, with most location estimates achieving primary azimuthal gaps between 165° and 270° (Figure 4i).

Discussion of Results

Figure 5 shows the earthquake epicenters recorded within the study area. The epicenters are depicted in different colors. Red epicenters with error ellipses are earthquake recorded by three or more seismic stations. The size and orientation of the error ellipse depends on the number of stations and epicenter geometry. Green epicenters are earthquakes recorded by only two stations. And yellow epicenters are earthquakes recorded by only one station. The spatial distribution of green epicenters corresponds to the distribution of red ones. The distribution of yellow epicenters is more chaotic. But most of these epicenters are also confined to seismically active regions.

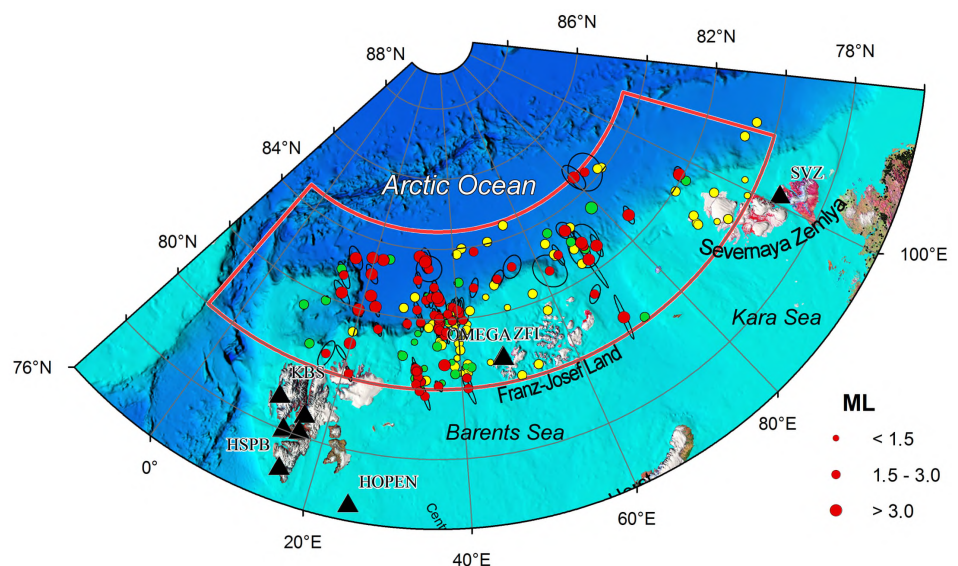


Figure 5. Bathymetric map (<https://www.ngdc.noaa.gov>) of the distribution of earthquakes (red circles) in the continent-ocean transition zone of the Eurasia Arctic region during the period from October 2011 to November 2020. The red line indicates the study area, and the black triangles indicate seismic stations.

The distribution of epicenters of the recorded earthquakes is not uniform over the area of study (Figure 5). The pronounced occurrence of the epicenters at negative morphostructures of the continental slope, namely, grabens and positive morphostructures –

highs should be noted. Most of the recorded earthquakes occurred at the Franz Victoria and St. Anna grabens, also at Kvitøya (Bely) island (Figure 6).

The earthquake epicenters recorded in the Franz Victoria graben area tend to occur in several parts of the graben area. Most epicenters are in the immediate vicinity of the continental slope, and at the boundary between the graben and the Bely and Victoria High, in its northern and southern parts (Figure 6).

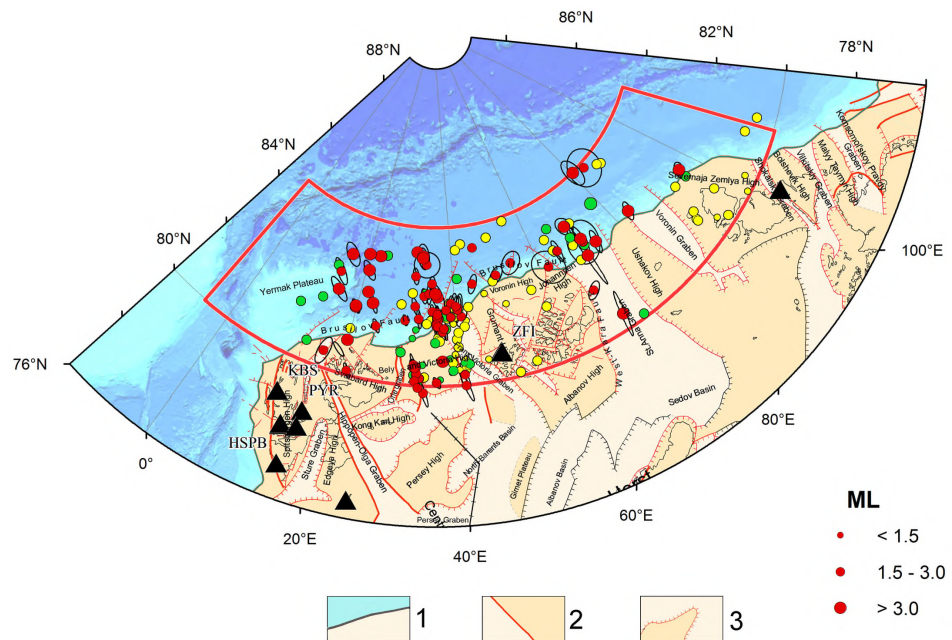


Figure 6. Map of the neotectonic structures and active faults [Alekseev, 2004] and distribution of earthquakes of the continent-ocean transition zone of the Eurasia Arctic region during the period from October 2011 to November 2020: 1-shelf edge, steep of flexure-fault zone; 2-main neotectonic faults; 3-dislocation with a break of continuity.

We relocated in [Morozov et al., 2018] the earthquakes occurring in the western sector of the Russian Arctic for the period from the early 20th century to 1989. It was shown that the Franz Victoria graben is one of the main seismically active areas of the Barents-Kara region. Seven earthquakes with $m_b(ISC) \geq 4.3$ had been recorded within the graben during the instrumental period (until 1989), while two events (1908 and 1948) had magnitudes 6.5 at the lowest; in particular, the 1908 earthquake had $M_w(ISC-GEM) = 6.6$ (Table 2). Earthquakes of smaller magnitude were not recorded in the Franz-Victoria Graben region due to the remoteness of seismic stations and their small number (Figure 1a). Thus, our results supplement the information about the seismicity features of this region.

The epicenters of the earthquakes recorded in the St. Anna graben area also tend to occur in several parts of the graben. Most epicenters are in the immediate vicinity of the continental slope. A few earthquakes are confined to the middle of the graben (Figure 5, 6).

West of the Franz Victoria graben is the Orle graben. Surveys conducted in the area showed an abnormally high heat flow at the graben, 300 to 520 mW/m² which is nearly 10 times the background value [Khutorskoi et al., 2009]. This anomalous heat flow is characteristic for the entire Orle graben and its extension in the continental slope up to a depth of 1200 m. [Khutorskoi et al., 2009] hypothesized crustal destruction in the graben area throughout its entire depth accompanied by the emplacement of hot mantle material, which provides evidence of an active phase in the graben evolution. High temperatures in the lithosphere can be invoked to explain a virtually complete absence of recorded earthquakes in the Orle graben area. Just two earthquakes can be supposed to have originated in the graben area. Further west, in the area of the Yermak Plateau, we have seismicity confined to the plateau slopes (Figure 6).

Table 2. Catalog of relocated seismic events in an area of the Franz Victoria Trench for the period from the beginning of the 20th century to 1989

Date dd.mm.yyyy	Time hh:mm:ss.0	Hypocenter			Error ellipse			Magnitude	Source of the hypocenter
		$\phi, ^\circ$	$\lambda, ^\circ$	$h^*,$ km	$Az_{major},$ °	$S_{minor},$ km	$S_{major},$ km		
14.10.1908	14:56:17.5	82.13	36.19	12f	100	87.0	193.0	$M_w(ISC) = 6.61$	by [Morozov et al., 2019]
18.02.1948	20:29:52.8	82.53	41.42	(0) 0–16	80	18.0	24.4	$M = 6.5$	by [Morozov et al., 2014]
26.09.1948	05:51:18.4	82.30	40.22	(4) 0–99	70	40.5	104.7	–	by [Morozov et al., 2014]
22.11.1948	23:32:48.0	82.42	41.90	(1) 0–65	90	25.8	38.1	–	by [Morozov et al., 2014]
13.03.1967	21:44:07.8	82.30	40.71	(0) 0–32	100	12.3	21.7	$m_b(ISC)=4.3$	by [Morozov et al., 2014]
14.03.1967	07:50:18.1	82.33	40.12	(4) 0–36	100	10.2	20.3	$m_b(ISC)=4.3$ $M(MOS)=5.5$	by [Morozov et al., 2014]
25.06.1975	10:14:57.9	82.42	39.54	(0) 0–43	100	14.1	35.5	$m_b(ISC)=4.6$ $m_b(NEIS)=4.6$ $M(LAO) = 4.8$	by [Morozov et al., 2014]

* – (h) means a fixed depth value when calculating the parameters of the epicenter; the number in brackets means the most probable depth value in the depth range.

From 2006 to 2009, researchers of the Geological Institute of the Russian Academy of Sciences, in collaboration with the Norwegian Petroleum Directorate, undertook three expeditions aimed at clarifying the structure of individual sections of the continent-ocean transition zone of the Barents Sea’s northwestern margins [Zaionchek et al., 2010]. These expeditions revealed a system of large landslides on the continental slope of the Arctic Ocean. Landslides had previously been found on the Norwegian continental slope, in the Litke graben and at the extension of the Hinlopen Strait [Hjelstuen et al., 2007; Vanneste et al., 2006; Winkelmann and Stein, 2007].

During one of the expeditions, signs of the intensive offset of large rock fragments of turbidite fracture and alluvial cone formation were detected inside the Orle graben formation. Similar phenomena were also observed on the western side, mainly occurring due to the isostatic compensation of avalanche sedimentation. It is therefore possible to assume that the eastern grabens, starting from the Franz Victoria, also act as channels for sedimentary material transport.

Researchers at the Kola Branch, GS RAS [Vinogradov and Baranov, 2013] studied the nature of seismic events in the western part of the Barents Sea shelf, within the continental slope area. Regarding minor seismicity ($M_L \leq 2.2$), seasonality was observed for the earthquakes registered in the area from the Strait of Storfjorden (Svalbard archipelago) to Bjornoya Island. In accordance with the suggested hypothesis, most of the low-magnitude earthquakes are the result of the landslide processes taking place in steep shelf areas, with their seasonality reflecting rapid changes in alluvial material mass flow during the warm season. In particular, by analyzing the records of the SPITS seismic group, the authors were able to identify waveforms caused by landslide events in the north of Spitsbergen.

Therefore, based on an overall analysis of the available geophysical, geotectonic and new seismic data, it can be assumed that the prevailing geodynamic factor responsible for the occurrence of low-magnitude earthquakes is the isostatic compensation of sedimentation in the continent-ocean transition zone.

Seismic activity is also observed within the easternmost island, Bely (Kvitøya) in the Svalbard archipelago, which also belongs to the Bely and Victoria High. On January 30, 2013, an earthquake with a magnitude of $M_L = 3.4$ occurred near Bely Island. After this earthquake, six earthquakes were recorded within five hours, which are aftershocks.

Disperse seismicity occurs in the area of Franz Josef Land and Severnaya Zemlya within the region of study. Since the time that a seismic station began operation on Severnaya Zemlya in 2016, some earthquakes have been recorded in the continental slope; however, the first thing to be noted consists in the fact that these were too few to infer definite occurrence at certain tectonic features. Secondly, nearly all events were located using records of a single station.

Conclusions

On the basis of the performed seismic monitoring of the continent-ocean transition zone of the Barents-Kara region during the period from October 2011 to November 2020, the following can be deduced:

1. A total of 192 earthquakes have been recorded during the period of observation with magnitudes in the range between 0.7 and 3.9. The pronounced occurrence of the epicenters at negative morphostructures of the continental slope, namely, grabens and positive morphostructures – highs should be noted.
2. The areas of highest seismicity are the Franz Victoria and St. Anna grabens and Bely and Victoria High. The prevailing geodynamic factor in the seismicity of the Franz Victoria and St. Anna grabens is most likely isostatic compensation of sedimentation in the continent-ocean transition zone.
3. The Orle graben is nearly free of earthquake occurrence. Surveys conducted in the Orle graben area showed an abnormally high heat flow at the graben, 300 to 520 mW/m², which is nearly 10 times the background value [Khutorskoi et al., 2009]. High temperatures in the lithosphere can be invoked to explain a virtually complete absence of recorded earthquakes in the Orle graben area.

Data and Resources

Access to the data from broadband stations operating in the Svalbard Archipelago was through the GEOFON program (HYPERLINK, <https://geofon.gfz-potsdam.de/waveform/>, visited on July, 2024). The bathymetry is from the National Geophysical Data Center and is available at https://www.ngdc.noaa.gov/mgg/bathymetry/maps/nos_intro.html (visited on July, 2024). Description of the AH network is available at DOI: <https://doi.org/10.7914/SN/AH>, the GE network – DOI: <https://doi.org/10.14470/TR560404>, the PL network – <https://www.fdsn.org/networks/detail/PL/> (visited on July, 2024), the NS network – DOI: <https://doi.org/10.7914/SN/NS>, the NO network – <https://www.fdsn.org/networks/detail/NO/> (visited on July, 2024), the II network – DOI: <https://doi.org/10.7914/SN/II>, the CN network – DOI: <https://doi.org/10.7914/SN/CN>, and the DK network – <https://www.fdsn.org/networks/detail/DK/> (visited on July, 2024).

Acknowledgments. The study was carried out under state contracts with N. Laverov Federal Center for Integrated Arctic Research of the Ural Branch of the Russian Academy of Sciences (project no. 122011300389-8), Schmidt Institute of Physics of the Earth of the Russian Academy of Sciences (project no. 075-00693-22-00), Geophysical Center of the Russian Academy of Sciences (project no. 075-00443-24-01), and Geophysical Survey of the Russian Academy of Sciences (state contract no. 075-00682-24, project no.122040800176-9).

References

- Akimov, A. P., and S. A. Krasilov (2020), Software complex WSG "Seismic Data Processing System". Certificate of state registration of the computer program No 2020664678 dated November 16, 2020 (in Russian), EDN: IJOVUE.
- Alekseev, M. N. (Ed.) (2004), *Atlas: geology and mineral resources of the shelf of Russia*, Geological Institute RAS (in Russian).
- Antonovskaya, G. N., N. K. Kapustian, Y. V. Konechnaya, and A. V. Danilov (2020), Registration Capabilities of Russian Island-Based Seismic Stations: Case Study of the Gakkel Ridge Monitoring, *Seismic Instruments*, 56(1), 33–45, <https://doi.org/10.3103/S0747923920010028>.

- Asming, V. E., A. V. Fedorov, A. N. Vinogradov, et al. (2016), The System of Automatic Seismological Monitoring of the North-West Russia and the Western Arctic, in *Modern Methods of Processing and Interpretation of Seismological Data. Proc. XI International Seismological Workshop. Kyrgyzstan, September 12-16*, pp. 34–36, GS RAS, Obninsk (in Russian).
- Avetisov, G. P. (1996), *Seismically active zones of the Arctic*, VNIIOkeangeologiya, St. Petersburg (in Russian).
- Engen, Ø., O. Eldholm, and H. Bungum (2003), The Arctic plate boundary, *Journal of Geophysical Research: Solid Earth*, 108(B2), <https://doi.org/10.1029/2002JB001809>.
- FDSN (2024), Arkhangelsk Seismic Network, <https://www.fdsn.org/networks/>, <https://doi.org/10.7914/SN/AH>, (visited on 07/31/2024).
- Fedorov, A. V., V. E. Asming, Z. A. Jevtjugina, and A. V. Prokudina (2019), Automated Seismic Monitoring System for the European Arctic, *Seismic Instruments*, 55(1), 17–23, <https://doi.org/10.3103/S0747923919010067>.
- Gabsatarova, I. P. (2006), Introduction into routine practice divisions of the Geophysical Survey of RAS calculation procedure of the local magnitude, in *MODERN METHODS OF PROCESSING AND INTERPRETATION OF SEISMOLOGICAL DATA. Materials from International seismological school dedicated to 100-anniversary foundation of seismic stations "Pulkovo" and "Ekaterinburg"*, pp. 49–53, GS RAS, Obninsk (in Russian).
- GFZ German Research Center for Geosciences (2021), GEOFON, <http://geofon.gfz-potsdam.de/geofon>, (visited on 07/31/2024).
- Gibbons, S. J., D. B. Harris, T. Dahl-Jensen, et al. (2017), Locating seismicity on the Arctic plate boundary using multiple-event techniques and empirical signal processing, *Geophysical Journal International*, 211(3), 1613–1627, <https://doi.org/10.1093/gji/ggx398>.
- Harboe, E. G. (1911), *Das Erdbebenobservatorium auf der Disko-Insel*, Gerlands Beiträge zur Geophysik.
- Havskov, J., P. Bormann, and J. Schweitzer (2002), Earthquake location, in *New Manual of Seismological Observatory Practice (NMSOP)*, Deutsches GeoForschungsZentrum GFZ.
- Hjelstuen, B. O., O. Eldholm, and J. I. Faleide (2007), Recurrent Pleistocene mega-failures on the SW Barents Sea margin, *Earth and Planetary Science Letters*, 258(3–4), 605–618, <https://doi.org/10.1016/j.epsl.2007.04.025>.
- International Seismological Centre (2024), Searching the ISC Bulletin, <https://doi.org/10.31905/D808B830>, (visited on 07/31/2024).
- Khutorskoi, M. D., Y. G. Leonov, A. V. Ermakov, and V. R. Akhmedzyanov (2009), Abnormal heat flow and the trough's nature in the Northern Svalbard plate, *Doklady Earth Sciences*, 424(1), 29–35, <https://doi.org/10.1134/S1028334X0910073>.
- Kremenetskaya, E., and V. Asming (2002), Problems of regional seismic event location and depth estimation in the European Arctic, *Workshop on IMS Location Calibration and Screening*, 4 (in Russian).
- Kulhánek, O. (1988), The status, importance, and use of historical seismograms in Sweden, in *Symposium on historical seismograms and earthquakes*, pp. 64–69, Academic Press.
- Kværna, T., and F. Ringdal (1996), Generalized Beamforming, Phase Association and Threshold Monitoring using a Global Seismic Network, in *Monitoring a Comprehensive Test Ban Treaty*, pp. 447–466, Springer Netherlands, https://doi.org/10.1007/978-94-011-0419-7_24.
- Morozov, A. N., and N. V. Vaganova (2017), The travel times of regional P and S for spreading ridges in the European Arctic, *Journal of Volcanology and Seismology*, 11(2), 156–163, <https://doi.org/10.1134/S0742046317020051>.
- Morozov, A. N., N. V. Vaganova, Y. V. Konechnaya, and V. E. Asming (2014), New data about seismicity and crustal velocity structure of the "continent-ocean" transition zone of the Barents-Kara region in the Arctic, *Journal of Seismology*, 19(1), 219–230, <https://doi.org/10.1007/s10950-014-9462-z>.
- Morozov, A. N., N. V. Vaganova, E. V. Ivanova, et al. (2016), New data about small-magnitude earthquakes of the ultraslow-spreading Gakkel Ridge, Arctic Ocean, *Journal of Geodynamics*, 93, 31–41, <https://doi.org/10.1016/j.jog.2015.11.002>.

- Morozov, A. N., N. V. Vaganova, V. E. Asming, Y. V. Konechnaya, and Z. A. Evtyugina (2018), The instrumental seismicity of the Barents and Kara sea region: relocated event catalog from early twentieth century to 1989, *Journal of Seismology*, 22(5), 1171–1209, <https://doi.org/10.1007/s10950-018-9760-y>.
- Morozov, A. N., N. V. Vaganova, and Y. V. Konechnaya (2019), The October 14, 1908 MW 6.6 earthquake in the Barents and Kara sea region of the Arctic: Relocation based on instrumental data, *Polar Science*, 20, 160–166, <https://doi.org/10.1016/j.polar.2019.05.001>.
- Panasenko, G. D. (1986), Problems of seismic zoning of the Western sector of the Soviet Arctic, in *Nature and economy of the North*, vol. 14, pp. 4–6, AS USSR, Geographical Society of the USSR, Northern Branch (in Russian).
- Peterson, J. R. (1993), *Observations and modeling of seismic background noise*, US Geological Survey, <https://doi.org/10.3133/ofr93322>.
- Rempp, G. (1914), *Aufstellung und Betrieb eines Seismographen auf der Deutschen Geophysikalischen Station Adventbai (Spitzbergen) 1911/12*, Gerlands Beiträge zur Geophysik.
- Rogozhin, E. A., G. N. Antonovskaya, N. K. Kapustian, and I. V. Fedorenko (2016), Features of seismicity of the Euro-Arctic region, *Doklady Earth Sciences*, 467(2), 389–392, <https://doi.org/10.1134/S1028334X16040140>.
- Schweitzer, J., B. Paulsen, G. N. Antonovskaya, et al. (2021), A 24-Yr-Long Seismic Bulletin for the European Arctic, *Seismological Research Letters*, 92(5), 2758–2767, <https://doi.org/10.1785/0220210018>.
- Vanneste, M., J. Mienert, and S. Bunz (2006), The Hinlopen Slide: A giant, submarine slope failure on the northern Svalbard margin, Arctic Ocean, *Earth and Planetary Science Letters*, 245(1–2), 373–388, <https://doi.org/10.1016/j.epsl.2006.02.045>.
- Vinogradov, A., and S. Baranov (2013), The possible impact of landslide processes on the seismicity of the North-Western part of the Barents sea, in *Modern methods of processing and interpretation of seismological data. Materials of the Eighth International Seismological Workshop*, pp. 99–103, GS RAS, Obninsk.
- Winkelmann, D., and R. Stein (2007), Triggering of the Hinlopen/Yermak Megaslide in relation to paleoceanography and climate history of the continental margin north of Spitsbergen, *Geochemistry, Geophysics, Geosystems*, 8(6), <https://doi.org/10.1029/2006GC001485>.
- Zaionchek, A., H. Brekke, S. Y. Sokolov, et al. (2010), The structure of the transition zone continent-ocean north-western periphery of the Barents Sea (according to 24, 25 and 26 flights vessel "Akademik Nikolai Strakhov" 2006–2009), in *The structure and evolution of the lithosphere*, pp. 111–157, Paulsen (in Russian).